Pathway of Incorporation of Microinjected Lamin A into the Nuclear Envelope

Anne E. Goldman, Robert D. Moir, Michelle Montag-Lowy, Murray Stewart,* and Robert D. Goldman

Department of Cell, Molecular and Structural Biology, Northwestern University Medical School, Chicago, Illinois 60611-3008; and *Medical Research Council Laboratory of Molecular Biology, Cambridge, United Kingdom

Abstract. When microinjected into the cytoplasm of 3T3 cells, biotinylated human lamin A rapidly enters the nucleus and gradually becomes incorporated into the nuclear lamina region as determined by immunofluorescence. The incorporation of the microinjected material takes several hours and progresses through a series of morphologically identifiable stages. Within minutes after microinjection, lamin A is found in spots distributed throughout the nucleus, except in nucleolar regions. Over a time course of up to 6 h, these spots appear to decrease in size and number as the biotinylated lamin A becomes associated with the endogenous nuclear lamina. Eventually, the typical nuclear rim staining pattern normally revealed by immunofluorescence with nuclear lamin antibodies is seen with antibiotin. This latter rim staining property is passed on to daughter cells following mitosis. These results indicate that the microinjected biotinylated nuclear lamin A retains those properties required for its integration into the lamina, as well as those necessary for the disassembly and subsequent reassembly of the nuclear lamina during cell division. The initial rapid accumulation into foci and the subsequent slower incorporation into the nuclear lamina appear to be analogous to the stages of incorporation following the microinjection of cytoskeletal intermediate filament proteins such as vimentin and keratin (Vikstrom, K., G. G. Borisy, and R. D. Goldman. 1989. *Proc. Natl. Acad. Sci. USA.* 86:549–553; Miller, R. K., K. Vikstrom, and R. D. Goldman. 1991. *J. Cell Biol.* 113: 843–855). Foci are also observed in some uninjected cells using nuclear lamin antibodies, indicating that these features are a genuine component of nuclear substructure. Evidence is presented that shows the appearance of these nuclear structures is cell cycle dependent.

THE nuclear lamina is a fibrous protein-rich layer that underlies the nuclear envelope, where it appears to interconnect nuclear pores and binds to receptors associated with the inner nuclear membrane (for reviews see Gerace and Burke, 1988; McKeon, 1991; Nigg, 1992). The lamina is thought to be involved both in organizing chromatin (Gerace and Burke, 1988; Yuan et al., 1991) and in DNA replication in interphase cells (Newport et al., 1990; Meier et al., 1991).

The nuclear lamins (NLs),[1] the major protein constituents of the nuclear lamina, show strong homology to cytoplasmic intermediate filament (IF) proteins (Nigg, 1992). The NL proteins have the characteristic IF central rod domain, in which there is a heptad repeat indicative of a coiled-coil conformation, together with globular NH_2- and COOH-terminal domains (McKeon, 1991). On the basis of this structural homology, NLs have been classified as type V IF proteins which are divided into two major subgroups on the basis of amino acid sequence and subcellular distribution during mitosis. One subgroup contains NL-A and NL-C which are "soluble" during cell division, whereas the other contains NL-B proteins which remain associated with lipid vesicles during mitosis (Nigg, 1992). Various NL isoforms have also been described. For example, up to five NLs have been reported in rat liver, including NL-A, NL-C, and three isoforms of NL-B (Kaufmann, 1989; see also Lehner et al., 1986). Variants of NL-B have been found in numerous different cell types of the same species, whereas NL-A and NL-C are found exclusively in differentiated cells (Nigg, 1992). Thus, several undifferentiated cell lines that express NL-B exclusively also express NL-A when induced to differentiate (Lebel et al., 1987; Kaufmann, 1989). On the other hand, there are species, such as the fruit fly *Drosophila* (Gruenbaum et al., 1988) and the clam *Spisula* (Dessev and Goldman, 1990), that appear to possess only a single NL protein.

Morphological studies using electron microscopy have revealed little information regarding the ultrastructure of the nuclear lamina in most cell types. Generally, all that is seen is a meshwork of fine fibrous material (Aaronson and Blobel, 1975), although, in rare instances, the lamina has been observed to have a well-organized structure. For example, a lattice-work of ~10-nm-diam filaments has been observed in the nuclear lamina of germinal vesicles of oocytes of *Xeno-*

1. *Abbreviations used in this paper*: IF, intermediate filament; MPF, maturation promoting factor; NL, nuclear lamin; snRNP, small RNP.

pus laevis (Aebi et al., 1986; Stewart and Whytock, 1988). In a recent light and electron microscope study of the structure of the lamina of HeLa cells, *Drosophila* embryos, and *Drosophila* cells in culture, three-dimensional reconstructions have indicated that the fibrillar network of the lamina covered no more than half the surface area of the inner nuclear membrane (Paddy et al., 1990).

Little is known about the molecular interactions of the various NL proteins in vivo. Most information on protein–protein interactions has been obtained from NL proteins studied in vitro. Cross-linking studies of isolated nuclei suggest that dimers are the major building blocks comprising the nuclear lamina, but other aggregates have also been detected (Dessev et al., 1990). Purified NL proteins form distinctive paracrystals in vitro (Aebi et al., 1986; Goldman et al., 1986; Heitlinger et al., 1991; Moir et al., 1991). Proteins prepared by expression in *E. coli* have been used to demonstrate that both the NH_2- and COOH-terminal globular domains of NL-A and -C influence their solubility and ability to form paracrystals (Moir et al., 1991). Furthermore, there appears to be a head-to-tail interaction of NL-B molecules during the early stages of paracrystal formation (Heitlinger et al., 1991). Other biochemical studies have suggested that the NH_2-terminal region of NL-A binds to the COOH-terminal region of NL-B (Georgatos et al., 1988). It should be pointed out, however, that the physiological significance of these in vitro studies remains unknown mainly because of the paucity of information regarding the in vivo structure of the nuclear lamina.

The nuclear lamina is an extremely insoluble structure that resists extraction except under conditions using high concentrations of salt or urea (Gerace et al., 1984). Despite this apparent stability in vitro, the lamina is rapidly disassembled and reassembled during cell division (Gerace and Blobel, 1980). The disassembly of the nuclear lamina is correlated with hyperphosphorylation of the NL proteins by the maturation promoting factor, MPF (Peter et al., 1990, 1991; Dessev et al., 1991). MPF is a complex containing the catalytic subunit, p34-cdc2 and cyclin B (Nurse, 1990). The NL phosphorylation sites for p34-cdc2 have been mapped and mutation of these sites affects the disassembly of the lamina in transfected cells and in in vitro assays (Heald and McKeon, 1990; Ward and Kirschner, 1990; Peter et al., 1991). There may be other NL sites phosphorylated by other kinases and it is not yet clear if phosphorylation is sufficient for lamin disassembly in vivo (Luscher et al., 1991). At the end of mitosis, the NL proteins are dephosphorylated and it has been proposed that they initiate nuclear envelope formation as they reassemble at the surface of decondensing chromosomes (Burke and Gerace, 1986; Burke, 1990; Glass and Gerace, 1990). However, recent evidence suggests that the nuclear lamins may not play such a direct role in the nuclear envelope reassembly process (Newport et al., 1990). Furthermore, cytoplasmic IF, specifically those containing type III proteins such as vimentin, are also phosphorylated by p34-cdc2, which appears to be sufficient for inducing their disassembly (Chou et al., 1990, 1991).

Recent studies on the properties of cytoplasmic IF suggest that during interphase they are dynamic, not static structures with respect to their ability to exchange subunits from a depolymerized to a polymerized state (Vikstrom et al., 1989). Data supporting these dynamic properties are derived from in vivo experiments in which soluble forms of biotinylated vimentin or keratin are injected into cells and are rapidly incorporated into their respective IF networks (Vikstrom et al., 1989; Mittal et al., 1989; Miller et al., 1991), as well as in vitro experiments using the method of fluorescence energy transfer (Angelides et al., 1989). In addition, the results of experiments using fluorescence recovery after photobleaching have suggested that a steady-state exchange mechanism exists between vimentin subunits and polymerized vimentin IFs in interphase cells (Vikstrom et al., 1992). Comparable experiments have yet to be carried out on the nuclear lamin system. As a result, very little is known about the properties of the interphase nuclear lamina, which may also be able to engage in similar exchanges of subunit proteins. Indeed, there must be molecular mechanisms responsible for the incorporation of NL proteins into the nuclear lamina to facilitate the increase in nuclear size after mitosis (Newport et al., 1990). Similar mechanisms may also underlie the increases in nuclear volume that take place when NL-A is incorporated into the lamina of differentiating lymphocytes (Kaufmann, 1989).

To more precisely address the molecular mechanisms regulating the assembly of the nuclear lamina and to develop more physiological assays for determining the functionality of NLs purified in vitro, we have initiated studies involving the microinjection of NL proteins. In this paper, we report the results obtained when human NL-A, made by expression of cDNA in *E. coli*, is injected into mouse 3T3 cells. After biotinylation, the injected protein can be localized by immunofluorescence. The labeled protein is transported rapidly from the cytoplasm into the nucleus and is then incorporated into the lamina in morphologically identifiable steps over a time course of several hours. The pathway of nuclear lamin assembly in interphase cells has revealed the presence of new nuclear structures. The results indicate that this method can be used to determine the dynamic properties and mechanisms involved in the assembly of the different types of NL proteins.

Materials and Methods

Expression and Purification of Human Lamin A

Human NL-A was obtained in milligram quantities by expression of the appropriate cDNA (the generous gift of Drs. Frank McKeon and Marc Kirschner; see McKeon et al., 1986) using a pET vector system based on a bacteriophage T7 promoter (Studier et al., 1990), as described in detail elsewhere (Moir et al., 1991). Expression of human NL-A required the presence of the pLysE plasmid (expressing lysozyme) to overcome leaky expression of T7 polymerase before induction with IPTG. The expressed protein was present in inclusion bodies isolated by standard methods (Nagai and Thogersen, 1987). Further purification was achieved by FPLC using a MonoS cation-exchanger column in 8 M urea, 20 mM Hepes, 1 mM EDTA, 1 mM DTT, pH 7.5, and a 0–1 M NaCl gradient. Column fractions containing NL-A were renatured by dialysis against 20 mM Tris-HCl, pH 8, 300 mM NaCl, 1 mM DTT. Paracrystals were formed by dialyzing renatured protein overnight against 20 mM MES, pH 6.5, 100 mM NaCl, 1 mM DTT (Moir et al., 1991).

Biotinylation of Human Lamin A

Biotinylation of NL-A was carried out using slight modifications of the protocol developed for labeling vimentin (Vikstrom et al., 1991). Paracrystals of purified NL-A were dissolved in 8 M urea, 20 mM Tris-HCl, pH 8.8, 2 mM DTT, 2 mM EDTA to give a final protein concentration of 1 mg/ml. 22 mM hydroxysuccinimidyl-D-biotin (Molecular Probes, Inc., Eugene,

OR) in dimethyl formamide (prepared as described in Vikstrom et al., 1991) was added to give a final concentration of 2.2 mM, and labeling was allowed to proceed for 30 min at room temperature. The reaction was then quenched by adding glycine to a final concentration of 80 mM. For microinjection, the protein was dialyzed against 20 mM Tris-HCl, pH 8.8, 500 mM NaCl, 2 mM DTT, 1 mM EDTA.

Cell Culture

Sparse cultures of mouse 3T3 cells (Todaro and Green, 1963) were grown on either 25-mm^2 photo-etched glass locator coverslips (Bellco Glass, Inc., Vineland, NJ) or on 22-mm^2 No. 1 coverslips in DME (Gibco Laboratories, Grand Island, NY), containing 10% bovine calf serum (Hyclone Laboratories Inc., Logan, UT), 50 U/ml penicillin, and 50 μg/ml streptomycin (Gibco Laboratories).

For studies of synchronized cells, mitotic 3T3 cells were obtained by mechanical shakeoff of subconfluent cultures grown in the absence of drugs using the method of Rosevear et al. (1990). Approximately 4×10^5 cells were obtained from 150-cm^2 culture flasks, of which at least 90% were mitotic. The cells were sedimented by centrifugation and washed with ice cold medium. Approximately 4×10^4 cells were placed on coverslips. These were fixed in methanol at −20°C at 1-h intervals after replating to obtain cells in the G1 phase of the cell cycle. Cells were also synchronized in S phase using methods described elsewhere (O'Keefe et al., 1992). Briefly, cells were plated at low density in serum-free medium for 52 h at which time all cells were in G-0 as indicated by the absence of mitotic figures. At this time the medium was replaced with medium containing 10% FCS for 4 h which induced the cells to enter G1. Hydroxyurea was then added to a final concentration of 1.5 mM for 16 h in order to block cells at the G1/S boundary. The cells were then released from this block by washing with and incubation in normal growth medium (see above), and subsequently fixed at 1-h intervals to obtain cells in various steps of S phase.

Microinjection Procedures

Micropipettes were made with borosilicate glass capillary tubing on a pipette puller (model 720; David Kopf Instrs., Tujunga, CA). Microinjections were performed on a Diavert inverted microscope (E. Leitz, Inc., Rockleigh, NJ) equipped with a Leitz micromanipulator. Biotinylated NL-A, at a concentration of ~0.8 mg/ml, was injected into the cytoplasm of 3T3 cells. The position of each injected cell was noted, and then the coverslips were placed in a CO_2 incubator and maintained at 37°C for varying time intervals. At appropriate times after injection, these preparations were fixed and processed for indirect immunofluorescence as described below.

Antibodies

Primary antibodies used in this study were goat antibiotin (Sigma Chemical Co., St. Louis, MO) and a rabbit antibody directed against BHK nuclear lamins, which were purified by paracrystal formation (Goldman et al., 1986) and SDS-PAGE. This antibody (anti-NL) reacted exclusively with the NL proteins by Western immunoblotting (data not shown). The secondary antibodies used were fluorescein-conjugated donkey anti-goat IgG and fluorescein-conjugated goat anti-rabbit IgG (Jackson ImmunoResearch Labs., Inc., West Grove, PA). For double-label immunofluorescence, rhodamine-conjugated donkey anti-rabbit IgG (Jackson ImmunoResearch Labs., Inc.) was used.

Light Microscopic Procedures

Cells grown on coverslips were fixed in cold methanol (−20°C), followed by air drying. Standard immunofluorescence techniques were carried out for single and double immunolabeling as described in detail elsewhere (Yang et al., 1985). Microinjected cells were identified on the locator coverslips by phase-contrast microscopy and were subsequently observed by epifluorescence on either a Zeiss Axiophot or Zeiss Laser Scan confocal microscope, using 40×, 63×, and 100× high NA objective lenses. Photomicrographs were recorded on 35-mm Plus-X film (Eastman Kodak Co., Rochester, NY).

Results

Microinjected Biotinylated Human Lamin A Is Incorporated into the Nuclear Lamina during Interphase

Mouse 3T3 cells were chosen as experimental models because they flatten extensively on their growth substrates and so provide optimal resolution of nuclear and cytoplasmic constituents. In most uninjected control cells prepared for indirect immunofluorescence using anti-NL, the nuclear lamina region was readily distinguished as a distinct perinuclear rim (Fig. 1). This rim staining is typical of that seen in a range of different cell types (Gerace et al., 1984).

Biotinylated human NL-A was microinjected into the

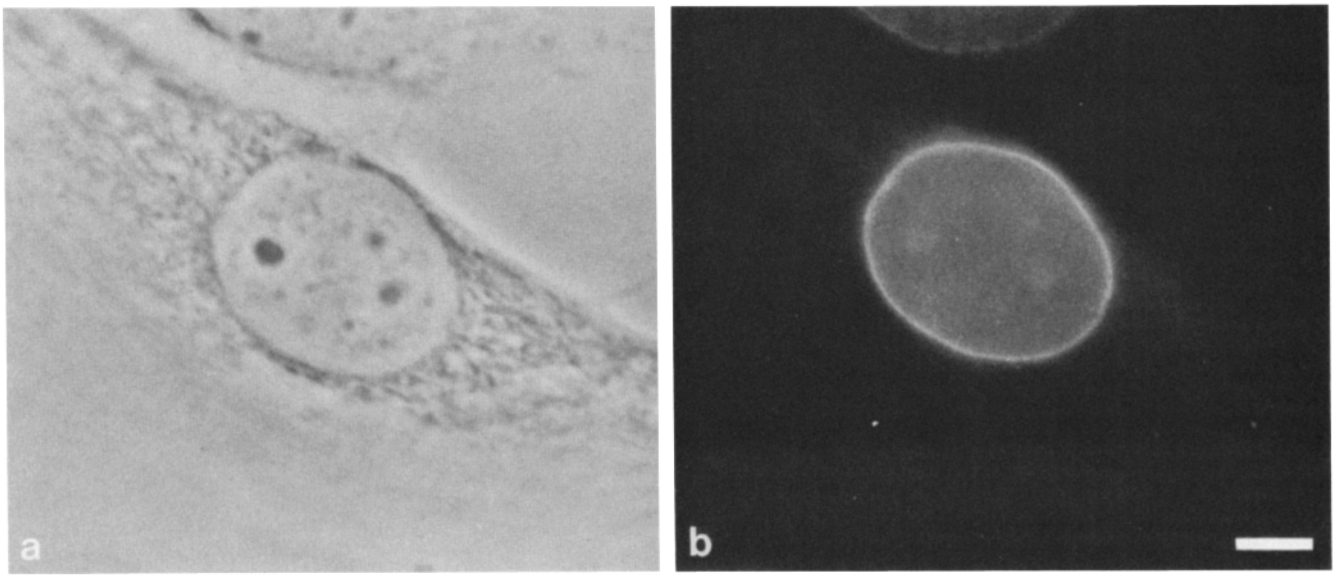

Figure 1. (*a* and *b*) A 3T3 cell displaying the typical interphase nuclear lamin pattern as revealed by indirect immunofluorescence with the rabbit antibody directed against nuclear lamins derived from BHK-21 cells. (*a*) Phase contrast; (*b*) the same cell viewed by immunofluorescence. Bar, 10 μm.

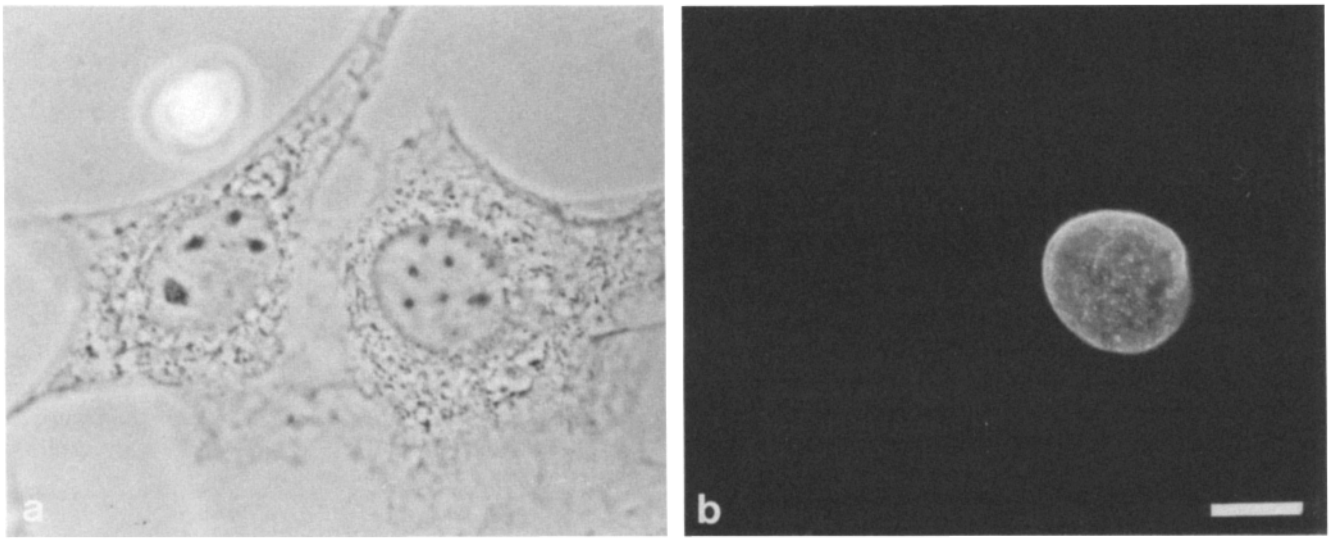

Figure 2. (*a* and *b*) A microscope field showing two 3T3 cells, one of which was injected with biotinylated lamin A, and subsequently fixed and stained for immunofluorescence at 6 h after injection. Note that only the injected cell fluoresces and and that, in addition to a bright rim, the nucleus also contains small spots. (*a*) Phase contrast; (*b*) fluorescence. Bar, 25 μm.

cytoplasm of mouse 3T3 cells growing on etched glass coverslips and incubated at 37°C. In our initial experiments, the coverslips were fixed and prepared for indirect immunofluorescence with antibiotin 5–6 h after injection (Fig. 2). The injected cells (Fig. 2 and 3 *e*) displayed a pattern very similar to that seen with NL antibodies in uninjected cells (Fig. 1). Thus, antibiotin staining was located at the nuclear periphery, although there was also some nucleoplasmic staining. This association of the biotinylated NL-A with the nuclear lamina indicated that the derivatized protein had retained the ability to integrate into the lamina. These observations also indicated that the nuclear lamin network in mouse 3T3 cells was capable of incorporating new NL protein subunits into its constituent polymeric structure during interphase.

Not All Antibiotin Staining Is Localized at the Nuclear Envelope

The majority of cells observed at 4–6 h after injection appeared as in Fig. 3 *e*, although the presence of a significant number of bright spots within nuclei of some injected cells was also apparent (Fig. 2 *b*). These spots which varied in size and number were much more apparent in cells observed at even shorter time intervals after injection. The observation of this novel nuclear morphology prompted us to investigate more carefully the distribution of endogenous lamins in uninjected cells to determine the extent to which such a distribution might reflect genuine structures found in vivo.

Some Uninjected Cells Also Show Punctate NL Staining in the Nucleus

As indicated above, most uninjected cells stained with anti-NL displayed the typical rim staining seen in Fig. 1. However, in actively growing cultures we also found a significant number of cells with prominent nuclear spots (Fig. 3 *f*), similar to those seen after microinjection and staining with antibiotin (Figs. 2 *b* and 3, *b–d*). This suggested that the pattern of spots we observed in microinjected cells was not simply an artifact arising from either microinjection or biotinylation, but instead reflected a genuine feature of the incorporation of lamins into the nuclear envelope (see cell synchronization section below). Based on these observations, we carried out a more extensive analysis of the pattern of incorporation of biotinylated NL-A at various time intervals after microinjection.

Pattern of Incorporation of Microinjected Human Lamin A

Biotinylated NL-A was injected into the cytoplasm of 3T3 cells and the position and time of injection for each cell was recorded. Coverslips were fixed at varying time intervals after injection and prepared for immunofluorescence with antibiotin. Within 2–5 min after injection, the majority of the fluorescence was located in the nuclear region (Fig. 3 *a*). Occasionally, a few spots could also be found in linear arrays in the cytoplasm (Fig. 3 *a*). After 30–180 min, all of the antibiotin staining was nuclear and mainly in the form of bright spots, variable in size, overlying a diffuse fluorescence background. At these early time points, relatively few spots appeared to be associated with the nuclear envelope and in general they were excluded from nucleolar regions (Figs. 3, *b–d*, and 4 *a*). Eventually, the largest spots disappeared and numerous smaller spots became apparent, some of which were lined up in the region of the nuclear envelope as shown by double indirect immunofluorescence (Fig. 4, *a–d*). These latter spots appeared to fuse and by 5–6 h after injection, most of the fluorescence was associated with the rim of the nucleus, and spots were reduced in number (Figs. 2 and 3 *e*). Double labeling with anti-NL also demonstrated that the endogenous lamina was not disrupted by the microinjection procedures (Fig. 4, *a–d*).

To determine more precisely the localization of the intranuclear spots containing biotinylated NL-A, injected cells were examined by confocal microscopy. The results showed that the spots were distributed throughout the nucleoplasm. This was seen at all time intervals after injection. For example, spots could be resolved in each focal plane of a through-

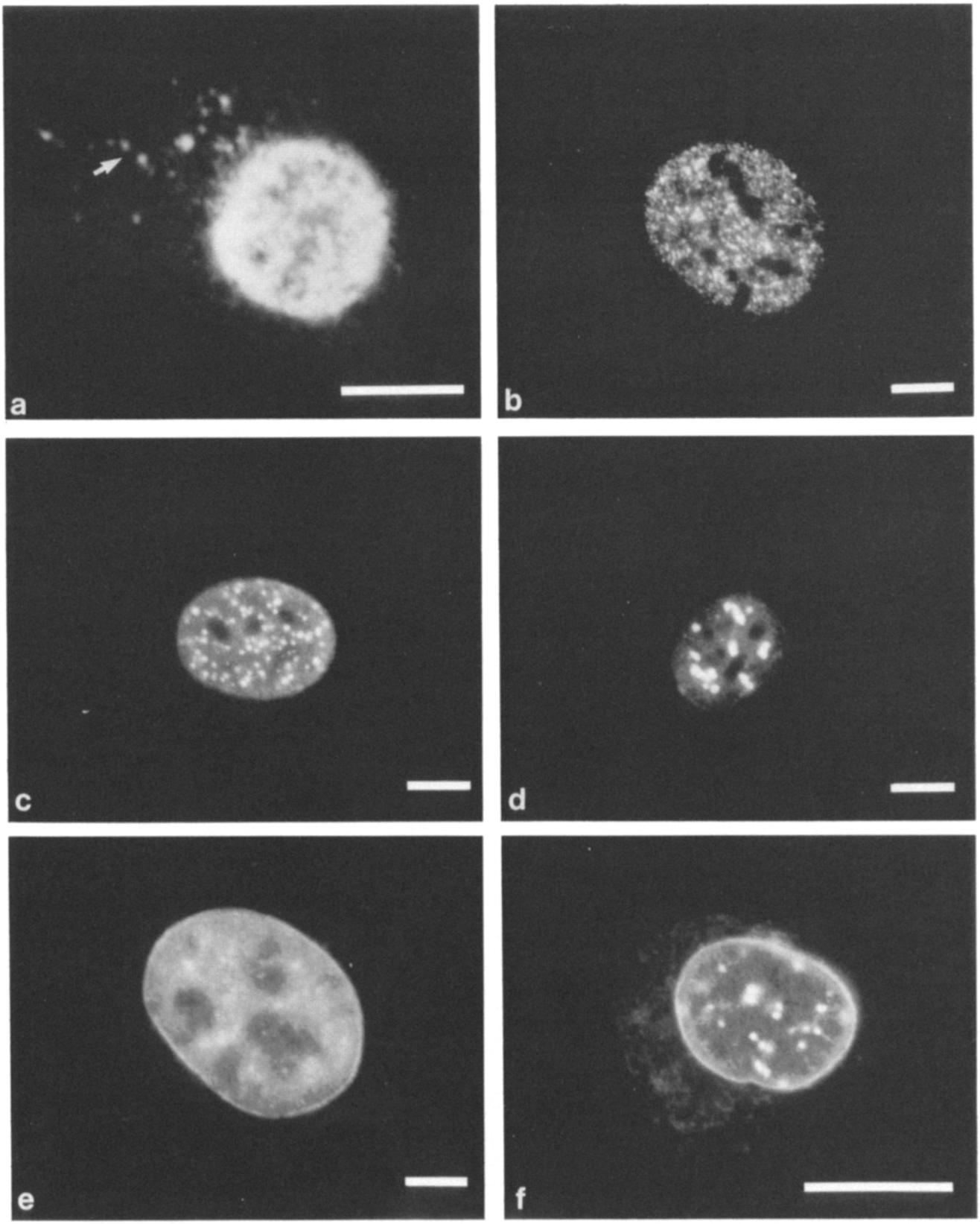

Figure 3. (*a*) A 3T3 cell fixed and prepared for indirect immunofluorescence with antibiotin at 5 min after microinjection with biotinylated lamin A. Most of the fluorescence is in the nuclear region, and the normally distinct boundary between the nucleus and the cytoplasm is not obvious. This latter observation suggests that a significant amount of human lamin A may be aggregated at the outer nuclear surface. Also note the array of bright cytoplasmic spots (*arrow*). These spots are usually not seen at later time intervals. Confocal optics. (*b–d*) 3T3 cells fixed and prepared for indirect immunofluorescence with antibiotin 30–180 min after injection with biotinylated lamin A. Within this time interval, the human lamin A is located in bright nuclear spots or foci that vary in size and number from cell to cell. At these postinjection times, the foci are rarely associated with the nuclear envelope and are excluded from the nucleolar regions. (*b*) 50 min; (*c*) 90 min; (*d*) 180 min. (*e*) A 3T3 cell observed at 5.5 h after injection with biotinylated human lamin A. Note the prominent fluorescent nuclear rim. (*f*) An uninjected 3T3 cell fixed and stained for immunofluorescence with nuclear lamin antibody. Note nuclear spots. Bars, (*a* and *f*) 25 μm; (*b–d*) 15 μm; (*e*) 10 μm.

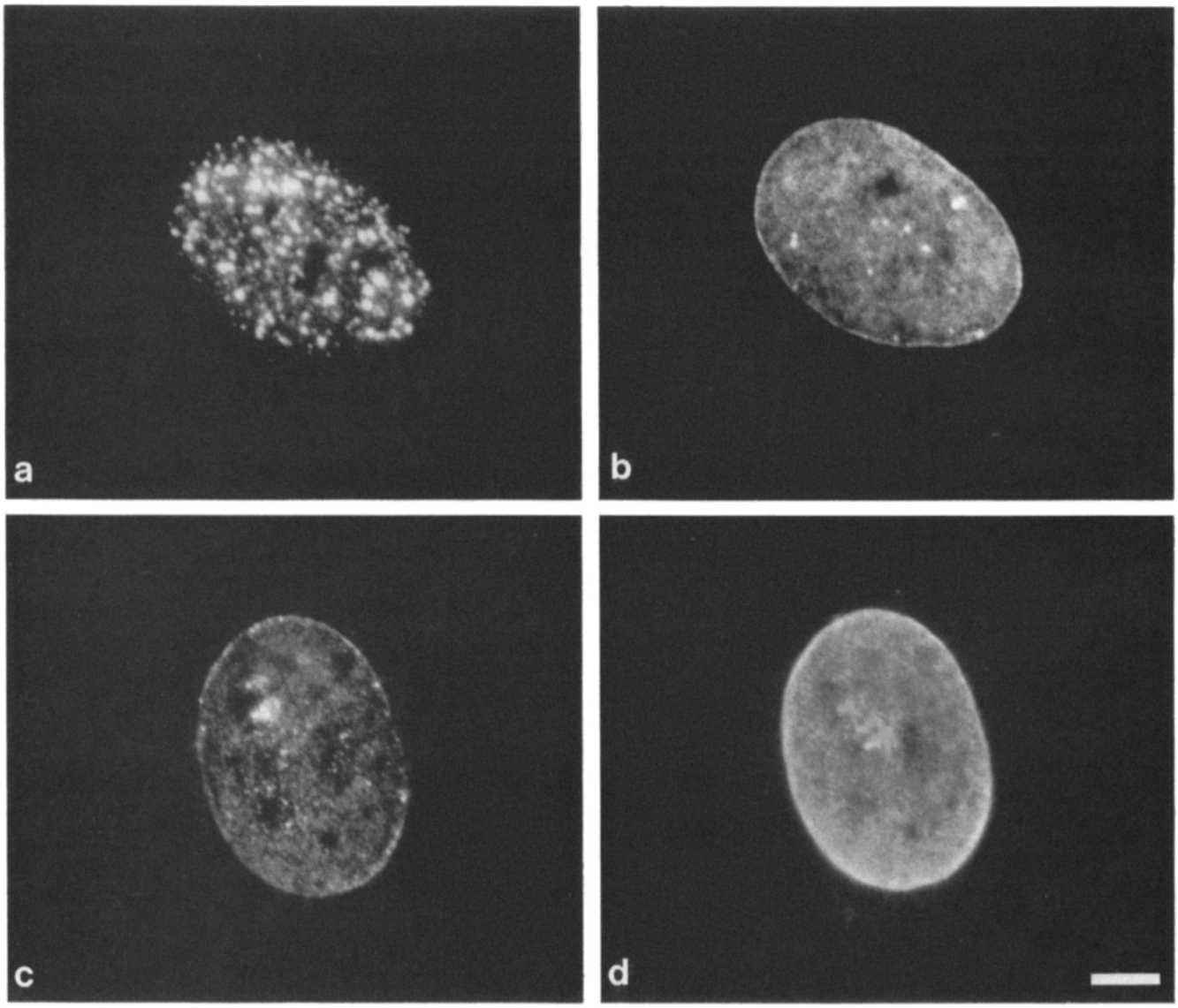

Figure 4. (*a* and *b*) 3T3 cell fixed 30 min after injection of biotinylated lamin A and prepared for double indirect immunofluorescence with (*a*) antibiotin and (*b*) anti-NL. The majority of the injected protein appears to be located within intranuclear spots at this timepoint, while the endogenous lamin network displays a typical interphase staining pattern with a prominent nuclear rim. (*c* and *d*) 3T3 cell fixed at 5.5 h after injection of biotinylated lamin A and prepared for double indirect immunofluorescence with (*c*) antibiotin and (*d*) anti-NL. The injected lamin A is now present in numerous smaller spots, some of which are lined up in the nuclear envelope region. Ultimately, these spots appear to fuse to form a nuclear rim very similar to that seen in Fig. 3 *e*. Please note that the spots containing biotinylated lamin A are not as apparent as might be expected in *b* and *d*. This is probably due to loss of contrast against the background of the normal nuclear lamina when stained with the complex polyclonal antibody which reacts with lamins A, B, and C. Bar, 10 μm.

focus series made at 90 min after injection. Furthermore, different patterns of nuclear spots were seen in different focal planes (Fig. 5, *a* and *b*). A similar distribution was seen in uninjected cells possessing nuclear spots after staining with anti-NL (Fig. 5, *c* and *d*).

Biotinylated Human Lamin A is Recognized and Distributed to Daughter Cells during Mitosis

Almost all cells incubated for 12–24 h after injection divided and both daughter cells exhibited a typical nuclear lamina staining pattern with antibiotin (Fig. 6). When newly divided cells were observed at relatively short times after microinjection, pairs of daughter cells could be found with nuclear spot patterns with antibiotin (Fig. 7). Uninjected cells containing the largest number of anti-NL staining spots were frequently found in pairs close to each other (Fig. 8), possibly indicating that they were newly divided daughter cells.

To test this latter possibility, we determined the numbers of cells containing nuclear spots in asynchronous growing cultures and in cells synchronized in G-O, G-1, G1/S, and S phase of the cell cycle. The results are presented in Table I. The data clearly indicate that almost half of the 3T3 cells in actively growing asynchronous cultures contain more than two nuclear spots. Furthermore there was a significant increase seen in cells containing nuclear spots in G-1. This elevated level of cells containing nuclear spots was also seen in G-O and in cells arrested at the G1/S boundary. This high percentage of cells with spots was maintained for up to 4 hours after cells entered S phase. However, by 4–6 h the

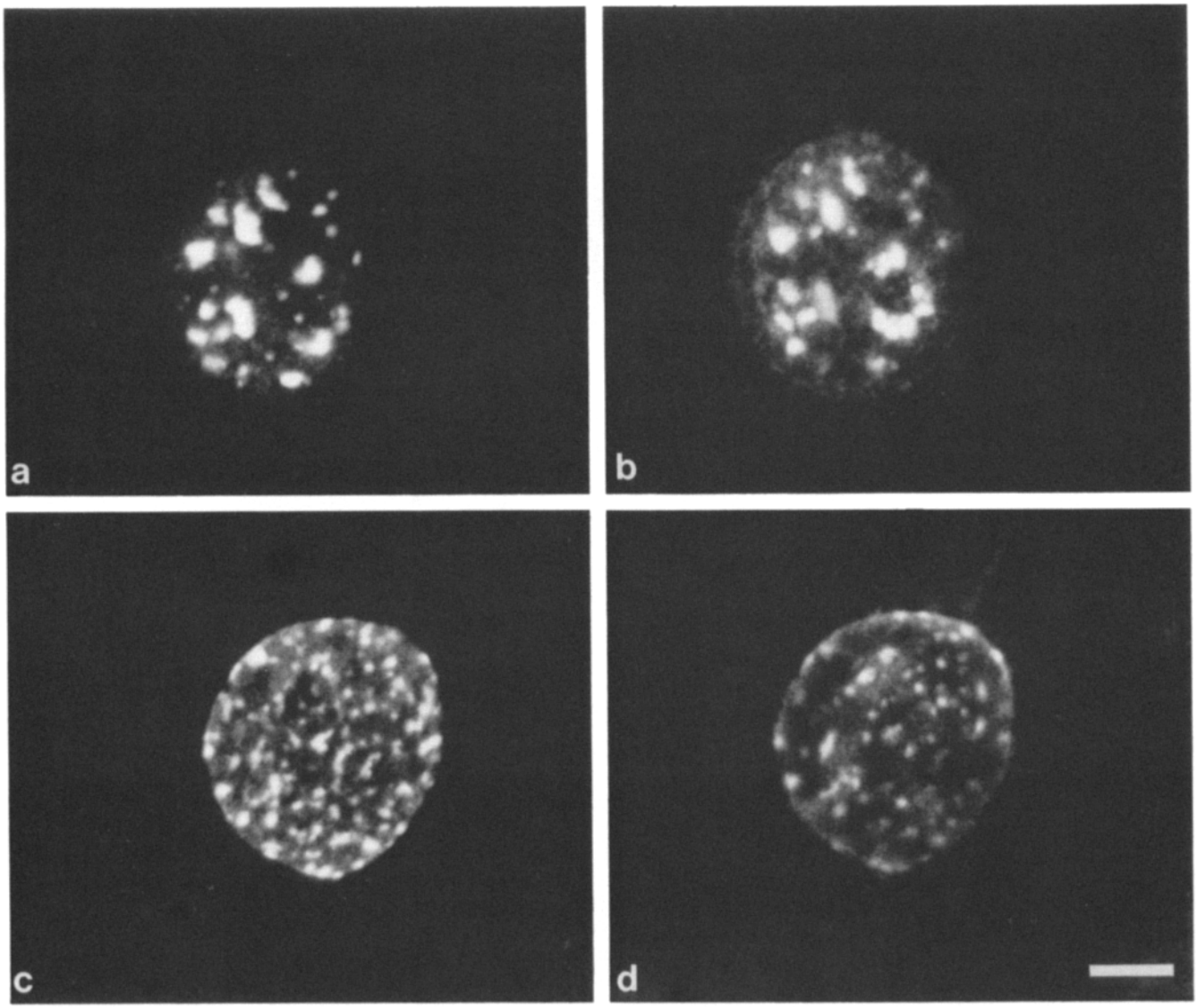

Figure 5. (*a* and *b*) A 3T3 cell fixed at 90 min after microinjection of biotinylated lamin A and processed for indirect immunofluorescence with antibiotin. These two micrographs were taken from a through focus series with the confocal microscope and are from focal planes within the nucleus which are ~1.5 μm apart. (*c* and *d*) Uninjected 3T3 cell fixed and prepared for indirect immunofluorescence with anti-NL. The spots present within the nucleus were examined by preparing a through focus series with the confocal microscope. These two micrographs are from focal planes within the nucleus that are 1.0 μm apart. Note that the bright spots appear to be distributed throughout the nucleoplasm as indicated by the different spot patterns in different focal planes. Bar, 10 μm.

number of cells with nuclear spots was significantly decreased to <50%.

Discussion

Microinjected Biotinylated NL-A Incorporates into the Nuclear Lamina

This study has demonstrated that microinjected biotinylated human NL-A retains the properties that permit it to become integrated into the endogenous nuclear lamina of mouse 3T3 cells. These results also demonstrate that the microinjected protein is targeted rapidly to the nucleus and little, if any, protein can be detected in the cytoplasm within a few minutes after microinjection. The behavior of biotinylated NL-A in cells that divide after microinjection further supports the idea that it retains the properties of endogenous lamins. In these cases, each daughter cell shows the staining of the nuclear periphery typically associated with the endogenous nuclear lamins (Gerace et al., 1984). This result shows that the derivatized NL-A is processed by 3T3 cells during mitosis and thereby indicates that the bacterially expressed biotinylated protein retains the essential features of NL-A required for incorporation into the nuclear lamina during interphase; disassembly during nuclear envelope breakdown on entering mitosis; and reformation of the nuclear lamina at the end of mitosis when the daughter cell nuclear envelopes reassemble (Nigg, 1992).

Rate of Incorporation

The rate of movement of microinjected biotinylated NL-A into the nucleus was extremely rapid and was usually com-

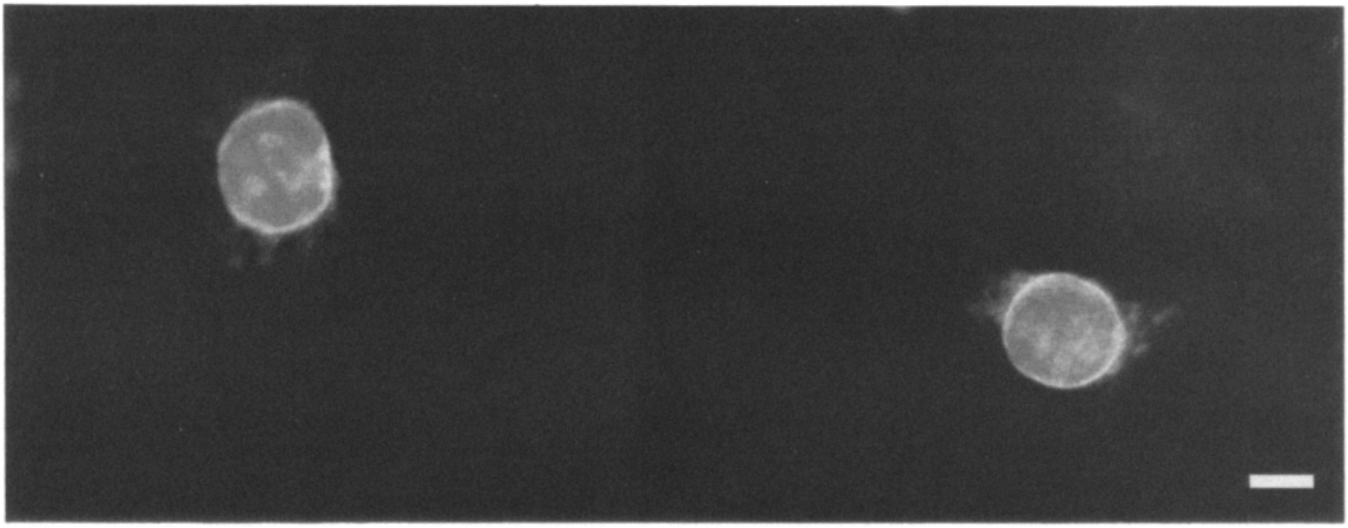

Figure 6. 3T3 cells fixed 20 h after microinjection of biotinylated lamin A and prepared for indirect immunofluorescence with antibiotin. The injected cell has divided and both daughter cells have characteristic nuclear rim staining patterns. Bar, 25 μm.

plete within a few minutes. In contrast, once inside the nucleus, the rate of incorporation of the microinjected protein into the nuclear lamina was much slower. It generally required several hours to begin to produce the nuclear rim staining typical of endogenous nuclear lamins, during which time the microinjected material progressed through several morphologically distinct stages. This unexpectedly slow time course of incorporation into the lamina may be related to a number of factors. For example, the slow rate of incorporation may be due to the state of saturation of the endogenous lamina. In this case, it would be necessary for new envelope synthesis to take place to enable the microinjected molecules to become incorporated. Alternatively, the extended time course of incorporation could reflect a slow rate of exchange between free lamin molecules in the nucleus and those polymerized in the lamina fibers. The apparent biochemical stability of the polymeric network comprising the lamina (Gerace et al., 1984) would be consistent with a slow off-rate of subunits, and therefore a slow rate of exchange between bound and "free" molecules. It is also possible that the slow rate of incorporation of the microinjected NL-A results from a requirement for biochemical modification or post-translational processing. For example, NL-A undergoes a series of COOH-terminal processing steps similar to those observed with ras-like G-proteins, including isoprenylation, removal of the three terminal amino acid residues, and methylation of the COOH-terminal cysteine residue (Nigg, 1992). These modifications are required for the targeting of NL-B to the inner aspects of the nuclear envelope (Krohne et al., 1989; Holtz et al., 1989; Kitten and Nigg, 1991), but it is not clear whether they take place in the nucleus or in the cytoplasm (Kitten and Nigg, 1991; Beck et al., 1990). Finally, it is also possible that incorporation of NL-A into the nuclear envelope is cell cycle dependent and that some stages of the cell cycle may even be refractory to its incorporation. This last possibility may ultimately explain at least part of the variation in incorporation rates we observed between different microinjected cells. Of course, these possibilities are not mutually exclusive, and it is likely that a combination of factors contributes to the rate of incorporation into the nuclear lamina of microinjected protein.

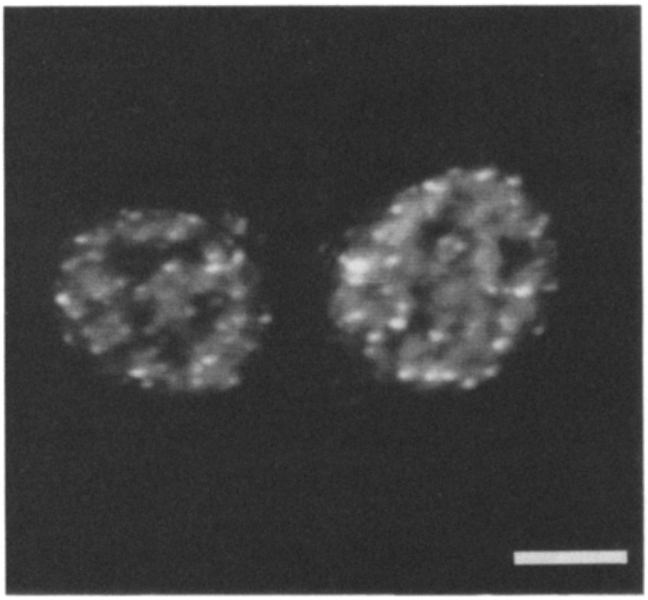

Figure 7. 3T3 cells fixed 5 h after microinjection of biotinylated lamin A and prepared for indirect immunofluorescence with antibiotin. Only one cell was injected. The close proximity of the two nuclei in adjacent cells suggests that the injected cell divided shortly before fixation. Nuclear spots are prominent in both nuclei. Confocal optics. Bar, 25 μm.

Intermediate Stages in NL-A Incorporation into the Nuclear Envelope

When biotinylated NL-A enters the nucleus, it is initially distributed widely through the nucleoplasm in discrete spots or foci as determined by both conventional fluorescence and confocal microscopy. Both the size and number of these nuclear spots vary from cell to cell, even when observed at the same time intervals after injection. These structures are not seen in close association with the nuclear envelope during early time intervals after injection. At later times, the spots

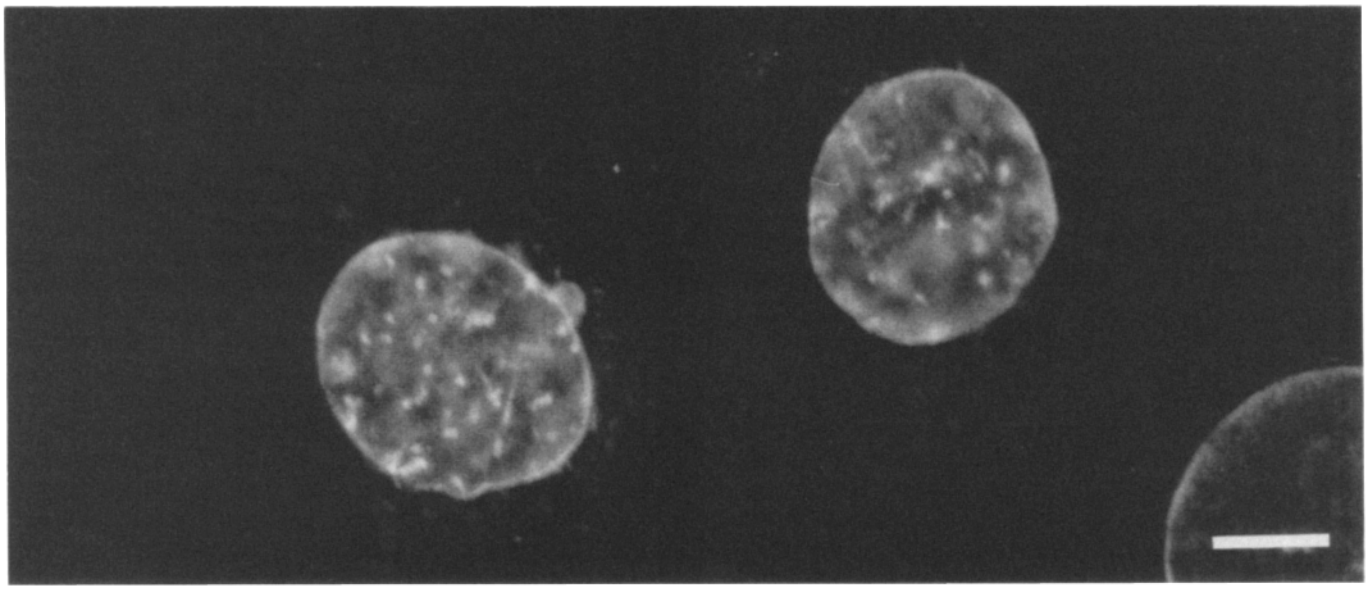

Figure 8. Uninjected 3T3 cells fixed and prepared for indirect immunofluorescence with anti-NL. The pair of cells were fixed soon after completion of mitosis and both daughter cell nuclei contain brightly staining nuclear spots. A portion of a more typical interphase nucleus is also evident in the lower right hand corner. Bar, 10 μm.

tend to become smaller and/or disappear and are seen in close association with the nuclear envelope. In the latter case, they frequently form punctate arrays. These arrays of small spots eventually appear to fuse, forming the typical nuclear lamin rim staining pattern.

The precise molecular structure of the intranuclear spots enriched with NL-A is unknown. A trivial explanation for these foci would be that they are nonspecific accumulations or condensations of an abnormally high concentration of free NL-A in the nucleus after microinjection. However, our observation of similar spots, in large numbers of noninjected interphase cells seen in asynchronous and synchronous cultures stained with nuclear lamin antibody, makes it unlikely that the foci form nonspecifically (see Table I). These NL-rich intranuclear structures are most prominent during those phases of the cell cycle in which nuclear growth and assembly processes are most likely to occur (e.g., G-1,S). It is also noteworthy that the cell cycle dependence of the nuclear lamin pattern may be related to the variability in intranuclear spot patterns seen at relatively short time intervals after the injection of biotinylated lamin A into asynchronous cells in culture (see Fig. 3).

The surface area of the nucleus is known to increase during cell growth and is proportional to total cell volume (Swanson et al., 1991). It is therefore likely that growth of the lamina is necessary to maintain this relationship (Newport et al., 1990). Consequently it is also likely that after mitosis, daughter cells transport newly synthesized nuclear lamin proteins rapidly into the nucleus, and it is plausible that such an elevated lamin concentration might result in the accumulation of lamins to form spots in a manner analogous to that which we have observed when an elevated nuclear concentration is induced by microinjection.

Based on the above considerations, the NL-A–rich foci seen in the nucleus after microinjection may be revealing endogenous nuclear substructures that are not visible in many interphase cells, especially those seen at longer time intervals after mitosis (e.g., 4–6 h or later after release of the G1/S block; see Table I). Thus, the microinjected NL-A may be concentrated at existing nuclear structures, making them

Table I. Fluorescence Microscopic Analyses of Nuclear Lamin Spots as a Function of the Cell Cycle

Observer	Asynchronous culture	Hours after replating mitotic cells (G-1)					Cells in G-O	Cells in G1/S	Hours after release from G1/S into S				
		1	2	3	4	6			1	2	3	4	6
1	47	46	48	77	56	73	74	73	68	68	70	39	43
2	51	56	76	74	67	78	78	62	66	71	58	20	60
3	56	68	80	77	67	85	78	74	64	75	89	45	55
4	37	50	58	44	44	49	65	58	54	70	68	35	26
Mean	48	55	71	68	59	71	74	67	63	71	71	35	46
SD	10	10	10	16	11	16	16	8	6	3	13	11	15

Summary of results from counts of nuclear lamin foci in asynchronous and synchronous cultures. Coverslips containing exponentially growing 3T3 cultures were fixed and stained with anti-NL to obtain the data for asynchronous cells. Cells were synchronized for the G1 observations by mitotic shakeoff and in G-0, G1/S, and S as described in Materials and Methods. 36–72 fluorescence micrographs were taken of random fields of each preparation using a 100×, 1.3 NA, planachromat objective. The micrographs were coded and examined "blind" by four different observers. Only nuclei with more than two "spots" were scored as positive. The number of positive nuclei at each stage is expressed as the percentage of total nuclei counted.

readily visible in the light microscope. It is also of interest that recent studies using lovastatin to inhibit isoprenylation showed some nuclear clumping of lamins (Lutz et al., 1992), which may be related to the foci seen after microinjection of biotinylated NL-A. These results would be consistent with the nuclear foci being associated with lamin processing.

The appearance at later time points of foci of biotinylated NL-A in close association with the endogenous nuclear envelope is also intriguing. Although at present we can only speculate on the possible significance of this observation for the detailed mechanism of nuclear lamina assembly, it is possible that these foci represent areas of incorporation of NL-A into the lamina. If such sites of incorporation represent areas of nuclear envelope synthesis, this observation could indicate that new envelope synthesis takes place at discrete locations at the nuclear surface. Another potential role for the foci at the nuclear envelope could be that they represent sites of further lamin processing. In addition to the COOH-terminal modifications discussed above, NL-A is proteolyzed to remove the COOH-terminal 18 residues after it is incorporated into the nuclear lamina (Gerace et al., 1984; Weber et al., 1989) and so the envelope-associated foci may represent the sites at which this proteolysis takes place.

The pattern of foci of NL is similar to the patterns seen with antibodies directed against components of small ribonucleoproteins (snRNPs). Both RNA and protein components of snRNPs, as well as splicing factors and pre-mRNA, have been localized to nucleoplasmic foci of varying sizes (Huang and Spector, 1992). The fundamental relationship between these different sized structures is not clear, but it has been suggested that small foci may be associated with interchromatin granules (proposed to be an accumulation of pre-mRNA transcripts) and perichromatin fibrils (sites of mRNP assembly), whereas larger foci are associated with coiled bodies that are thought to be derived from nucleoli (Fu and Maniatis, 1990; Raska et al., 1990; Carmo-Fonseca et al., 1991*a*,*b*; Wang et al., 1991; Carter et al., 1991). "Punctate foci" (Saunders et al., 1991) and nuclear dots (Ascoli and Maul, 1991) that are distinct from RNP foci have also been described. The existence of these various structures implies that the interphase nucleus is organized into domains. It will be of interest in the future to determine the structural and spatial relationships of these nuclear structures with those seen with lamin antibodies.

Analogies to Cytoplasmic Intermediate Filament Proteins

Previous studies using biotinylated IF proteins such as vimentin (Vikstrom et al., 1989) and type I keratin (Miller et al., 1991) have demonstrated the formation of cytoplasmic spots morphologically comparable to the NL-A nuclear spots immediately after microinjection. The keratin and/or vimentin in these spots becomes incorporated into the endogenous IF network over a time course of 30 min to 3 h. Therefore, the time course for incorporation of microinjected cytoplasmic IF proteins is similar to NL-A with respect to the nuclear lamina. Spots enriched in vimentin containing profilaments are also seen in mitotic BHK-21 cells. During the later stages of mitosis, the proteinaceous aggregates disappear as the normal interphase IF network reappears (Rosevear et al., 1990). These various observations suggest that the formation of foci represent normal intermediate steps in the assembly of both nuclear and cytoplasmic IF networks.

Transport of Microinjected NL-A

The initial transport of microinjected NL-A from the cytoplasm to the nucleus is remarkably rapid, being essentially complete in ~5 min. Clearly this movement is far more rapid than could be accounted for by simple diffusion. Therefore, it seems likely that some form of active cytoplasmic transport, probably involving unknown molecular motors as well as a specific tracking system, is responsible for this accumulation. In addition, the gradual translocation of foci from the nuclear matrix to the nuclear lamina also raises the question of an active transport mechanism within the nucleus.

We thank Satya Khuon for her excellent technical assistance and Laura Davis for her help in preparing the manuscript. We also wish to acknowledge the help of Dr. Norman Rushforth with the statistical analysis of the data presented in Table I.

This work has been supported by National Cancer Institute grant CA31760-11.

Received for publication 17 April 1992 and in revised form 12 August 1992.

Note added in proof: It has come to our attention that a paper will be published in the near future in which similar intranuclear lamin rich foci are described in human fibroblasts. The reference is as follows: Bridger, J. M., I. R. Kill, M. O'Farrell, and C. J. Hutchison. 1993. Internal lamin structures within G-1 nuclei of human dermal fibroblasts. *J. Cell. Sci.* In press.

References

Aaronson, R. P., and G. Blobel. 1975. Isolation of nuclear pore complexes in association with a lamina. *Proc. Natl. Acad. Sci. USA.* 72:1007–1011.

Aebi, U., J. Cohn, L. Buhle, and L. Gerace. 1986. The nuclear lamina is a meshwork of intermediate filaments. *Nature (Lond.).* 323:560–564.

Angelides, K. J., K. E. Smith, and M. Takeda. 1989. Assembly and exchange of intermediate filament proteins of neurons: Neurofilaments are dynamic structures. *J. Cell Biol.* 108:1074–1084.

Ascoli, C., and G. Maul. 1991. Identification of a novel nuclear domain. *J. Cell Biol.* 112:785–795.

Beck, L. A., T. J. Hosik, and M. Sinensky. 1990. Isoprenylation is required for the processing of the lamin A precursor. *J. Cell Biol.* 110:1489–1499.

Burke, B. 1990. On the cell-free association of lamins A and C with metaphase chromosomes. *Exp. Cell Res.* 186:169–176.

Burke, B., and L. Gerace. 1986. A cell-free system to study reassembly of the nuclear envelope at the end of mitosis. *Cell.* 44:639–652.

Carmo-Fonseca, M., R. Pepperkok, B. S. Sproat, W. Ansorge, M. S. Swanson, and A. Lamond. 1991*a*. *In vivo* detection of SnRNP-rich organelles in the nuclei of mammalian cells. *EMBO (Eur. Mol. Biol. Organ.) J.* 10: 1863–1873.

Carmo-Fonseca, M., D. Tollervey, R. Pepperkok, S. M. L. Barabino, A. Mardes, C. Brunner, P. D. Zamore, M. R. Green, E. Hurt, and A. I. Lamond. 1991*b*. Mammalian nuclei contain foci which are highly enriched in components of the pre-mRNA splicing machinery. *EMBO (Eur. Mol. Biol. Organ.) J.* 10:195–206.

Carter, K. C., K. L. Tuneja, and J. B. Lawrence. 1991. Discrete nuclear domains of poly (A) RNA and their relationship to the functional organization of the nucleus. *J. Cell Biol.* 115:1191–1202.

Chou, Y.-H., J. R. Bischoff, D. Beach, and R. D. Goldman. 1990. Intermediate filament reorganization during mitosis is mediated by $p34^{cdc2}$ phosphorylation of vimentin. *Cell.* 62:1063–1071.

Chou, Y.-H, K.-L Ngai, and R. D. Goldman. 1991. The regulation of intermediate filament reorganization in mitosis: $p34^{cdc2}$ phosphorylates vimentin at a unique N-terminal site. *J. Biol. Chem.* 266:7325–7328.

Dessev, G., and R. D. Goldman. 1990. The oocyte lamin persists as a single major component of the nuclear lamina during embryonic development of the surf clam. *Int. J. Dev. Biol.* 34:267–274.

Dessev, G., C. Iovcheva-Dessev, and R. D. Goldman. 1990. Lamin dimers: presence in the nuclear lamina of surf clam oocytes and release during nuclear envelope breakdown. *J. Biol. Chem.* 265:12636–12641.

Dessev, G., C. Iovcheva-Dessev, J. R. Bischoff, D. Beach, and R. D. Gold-

man. 1991. A complex containing $p34^{cdc2}$ and cyclin B phosphorylates the nuclear lamin and disassembles nuclei of clam oocytes in vitro. *J. Cell Biol.* 112:523–533.

Fu, V., and T. Maniatis. 1990. Factor required for mammalian spliceosome assembly is localized in discrete regions in the nucleus. *Nature (Lond.).* 343: 437–441.

Georgatos, S. D., C. Stournaras, G. Blobel. 1988. Heterotypic and homotypic associations between the nuclear lamins: site-specificity and control by phosphorylation. *Proc. Natl. Acad. Sci. USA.* 85:4325–4329.

Gerace, L., and G. Blobel. 1980. The nuclear envelope is reversibly depolymerized during mitosis. *Cell.* 19:277–287.

Gerace, L., and B. Burke. 1988. Functional organization of the nuclear envelope. *Annu. Rev. Cell Biol.* 4:335–374.

Gerace, L., C. Comeau, and M. Benson. 1984. Organization and modulation of nuclear structure. *J. Cell Sci. Suppl.* 1:137–160.

Glass, J. R., and L. Gerace. 1990. Lamins A and C bind and assemble at the surface of mitotic chromosomes. *J. Cell Biol.* 111:169–176.

Goldman, A. E., G. Maul, P. M. Steinert, H.-Y. Yang, and R. D. Goldman. 1986. Keratin-like proteins that coisolate with intermediate filaments of BHK-21 cells are nuclear lamins. *Proc. Natl. Acad. Sci. USA.* 83:3839–3843.

Gruenbaum, Y., Y. Landesman, B. Drees, J. W. Bare, H. Saumweber, M. R. Paddy, J. W. Sedat, D. E. Smith, B. M. Benton, and P. A. Fisher. 1988. Drosophila nuclear lamin Precursor Dm0 is translated from either of two developmentally regulated mRNA species apparently encoded by a single gene. *J. Cell Biol.* 106:585–596.

Heald, R., and F. McKeon. 1990. Mutations of phosphorylation sites in lamin A that prevent nuclear lamina disassembly in mitosis. *Cell.* 61:579–589.

Heitlinger, E., M. Peter, M. Haner, A. Lustig, U. Aebi, and E. A. Nigg. 1991. Expression of chicken lamin B2 in *Escherichia coli*: characterization of its structure, assembly, and molecular interactions. *J. Cell Biol.* 113:485–495.

Holtz, D., R. A. Tanaka, J. Hartwig, and F. McKeon. 1989. The CaaX motif of lamin A functions in conjunction with the nuclear localization signal to target assembly to the nuclear envelope. *Cell.* 59:969–977.

Huang, S., and D. L. Spector. 1992. U1 and U2 small nuclear RNAs are present in nuclear speckles. *Proc. Natl. Acad. Sci. USA.* 89:305–308.

Kaufmann, S. 1989. Additional members of the rat liver lamin polypeptide family. *J. Biol. Chem.* 264:13946–13955.

Kitten, G. T., and E. A. Nigg. 1991. The CaaX motif is required for isoprenylation, carboxyl methylation, and nuclear membrane association of lamin B_2. *J. Cell Biol.* 113:13–23.

Krohne, G., I. Waizeneger, and T. H. Hoger. 1989. The conserved carboxy-terminal cysteine of nuclear lamins is essential for lamin association with the nuclear envelope. *J. Biol. Chem.* 109:2003–2011.

Lebel, S., C. Lampron, C. A. Royal, and Y. Raymond. 1987. Lamins A and C appear during retinoic acid-induced differentiation of mouse embryonal carcinoma cells. *J. Cell Biol.* 105:1099–1104.

Lehner, C. F., V. Kurer, H. M. Eppenberger, and E. A. Nigg. 1986. The nuclear lamin family in higher vertebrates: identification of quantitatively minor lamin proteins by monoclonal antibodies. *J. Biol. Chem.* 261:13293–13301.

Luscher, B., L. Brizuela, D. Beach, and R. N. Eisenman. 1991. A role for the $p34^{cdc2}$ kinase and phosphatases in the regulation and disassembly of lamin B2 during the cell cycle. *EMBO (Eur. Mol. Biol. Organ.) J.* 10:865–875.

Lutz, R. J., M. A. Trujillo, K. S. Denham, L. Wenger, and M. Sinensky. 1992. Nucleoplasmic localization of pre-lamin A: implications for prenylation-dependent lamin A assembly into the nuclear lamina. *Proc. Natl. Acad. Sci. USA.* 89:3000–3004.

McKeon, F. D. 1991. Nuclear lamin proteins: domains required for nuclear targeting, assembly, and cell-cycle regulated dynamics. *Curr. Opin. Cell Biol.* 3:82–86.

McKeon, F. D., M. W. Kirschner, and D. Caput. 1986. Homologies in both primary and secondary structure between nuclear envelope and intermediate filament proteins. *Nature (Lond.).* 319:463–468.

Meier, J., K. H. S. Campbell, C. C. Ford, R. Stick, and C. J. Hutchison. 1991. The role of lamin LIII in nuclear assembly and DNA replication, in cell-free extracts of *Xenopus* eggs. *J. Cell Sci.* 98:271–279.

Miller, R. K., K. Vikstrom, and R. D. Goldman. 1991. Keratin incorporation into intermediate filaments is a rapid process. *J. Cell Biol.* 113:843–855.

Mittal, B., J. M. Sanger, and J. W. Sanger. 1989. Visualisation of intermediate filaments in living cells using fluorescently labeled desmin. *Cell Motil. Cytoskeleton.* 12:127–138.

Moir, R. D., A. D. Donaldson, and M. Stewart. 1991. Expression in *Escherichia coli* of human lamins A and C: influence of head and tail domains on assembly properties and paracrystal formation. *J. Cell Sci.* 99:363–372.

Nagai, K., and. H.-C. Thogersen. 1987. Synthesis and sequence-specific proteolysis of hybrid proteins produced in *Escherichia coli. Methods Enzymol.* 153:461–481.

Newport, J., K. L. Wilson, and W. G. Dunphy. 1990. A lamin-independent pathway for nuclear envelope assembly. *J. Cell Biol.* 111:2247–2259.

Nigg, E. 1992. Assembly-disassembly of the nuclear lamina. *Curr. Opin. Cell Biol.* 4:105–109.

Nurse, P. 1990. Universal control mechanism regulating the onset of M phase. *Nature (Lond.).* 344:503–508.

O'Keefe, R. T., S. C. Henderson, and D. L. Spector. 1992. Dynamic organization of DNA replication in mammalian cell nuclei spatially and temporally defined replication of chromosome-specific satellite DNA sequences. *J. Cell Biol.* 116:1095–1110.

Paddy, M. R., A. S. Belmont, H. Saumweber, D. A. Agard, and J. W. Sedat. 1990. Interphase nuclear envelope lamins form a discontinuous network that interacts with only a fraction of the chromatin in the nuclear periphery. *Cell.* 62:89–106.

Peter, M., J. Nakagawa, M. Doree, J. C. Labbe, and E. A. Nigg. 1990. *In vitro* disassembly of the nuclear lamina and M phase–specific phosphorylation of lamins by cdc2 kinase. *Cell.* 61:591–602.

Peter, M., E. Heitlinger, M. Haner, and E. A. Nigg. 1991. Disassembly of *in vitro* formed head-to-tail polymers by cdc2 kinase. *EMBO (Eur. Mol. Biol. Organ.) J.* 10:1535–1544.

Raska, I., R. L. Ochs, L. E. C. Andrade, E. K. L. Chan, R. Burlingame, C. Peebes, D. Gruol, and E. M. Tan. 1990. Association between the nucleolus and the coiled body. *J. Struct. Biol.* 104:120–127.

Rosevear, E. R., M. McReynolds, and R. D. Goldman. 1990. Dynamic properties of intermediate filaments: disassembly and reassembly during mitosis in baby hamster kidney cells. *Cell Motil. Cytoskeleton.* 17:150–166.

Saunders, W. S., C. A. Cooke, and W. C. Earnshaw. 1991. Compartmentalization within the nucleus: discovery of a novel subnuclear region. *J. Cell Biol.* 115:919–931.

Stewart, M., and S. Whytock. 1988. The structure and interactions of components of nuclear envelopes of *Xenopus* oocyte germinal vesicles observed by heavy metal shadowing. *J. Cell Sci.* 90:409–423.

Studier, F. W., A. W. Rosenberg, J. J. Dunn, and J. W. Dubendorff. 1990. Use of T7 polymerase to direct expression of cloned genes. *Methods Enzymol.* 185:60–89.

Swanson, J., M. Lee, and P. E. Knapp. 1991. Cellular dimensions affecting nucleocytoplasmic volume ratio. *J. Cell Biol.* 115:941–948.

Todaro, G., and H. Green. 1963. Quantitative studies of the growth of mouse embryo cells in culture and their development into established lines. *J. Cell Biol.* 17:299–313.

Vikstrom, K., G. G. Borisy, and R. D. Goldman. 1989. Dynamic aspects of intermediate filament networks in BHK-21 cells. *Proc. Natl. Acad. Sci. USA.* 86:549–553.

Vikstrom, K. L., R. K. Miller, and R. D. Goldman. 1991. Analyzing dynamic properties of intermediate filaments. *Methods Enzymol.* 196:506–525.

Vikstrom, K. L., S. Lim, R. D. Goldman, and G. G. Borisy. 1992. Steady state dynamics of intermediate filament networks. *J. Cell Biol.* 118:121–129.

Wang, J., L. G. Cao, Y.-L. Wang, and T. Pederson. 1991. Localization of premessenger RNA at discrete nuclear sites. *Proc. Natl. Acad. Sci. USA.* 79:7391–7395.

Ward, G. E., and M. W. Kirschner. 1990. Identification of cell cycle regulated phosphorylation sites on nuclear lamin C. *Cell.* 61:561–577.

Weber, K., U. Plessmann, and P. Traub. 1989. Maturation of nuclear lamin A involves a specific carboxy-terminal trimming which removes the polyisoprenylation site from the precursor implications for the nuclear lamina. *FEBS Lett.* 257:4111–4114.

Yang, H.-Y., N. Lieska, A. E. Goldman, and R. D. Goldman. 1985. A 300,000-mol wt intermediate filament-associated protein in BHK-21 cells. *J. Cell Biol.* 100:620–631.

Yuan, J., G. Simos, G. Blobel, and S. D. Georgatos. 1991. Binding of lamin A to polynucleosomes. *J. Biol. Chem.* 266:9211–9215.